Particle Rotation Effects in Rarefied Two-Phase Plume Flows

Jonathan M. Burt and Iain D. Boyd

Department of Aerospace Engineering
University of Michigan, Ann Arbor, MI 48109

Abstract. We evaluate the effects of solid particle rotation in high-altitude solid rocket exhaust plume flows, through the development and application of methods for the simulation of two phase flows involving small rotating particles and a nonequilibrium gas. Green's functions are derived for the force, moment, and heat transfer rate to a rotating solid sphere within a locally free-molecular gas, and integration over a Maxwellian gas velocity distribution is used to determine the influence of particle rotation on the heat transfer rate at the equilibrium limit. The use of these Green's functions for the determination of particle phase properties through the Direct Simulation Monte Carlo method is discussed, and a procedure is outlined for the stochastic modeling of interphase collisions. As a test case, we consider the nearfield plume flow for a Star-27 solid rocket motor exhausting into a vacuum, and vary particle angular velocities at the nozzle exit plane in order to evaluate the influence of particle rotation on various flow properties. Simulation results show that rotation may lead to slightly higher particle temperatures near the central axis, but for the case considered the effects of particle rotation are generally found to be negligible.

INTRODUCTION

In the modeling and analysis of exhaust plumes from solid-propellant rockets, several complex and poorly understood physical phenomena are often overlooked. In particular, the Al_2O_3 particles which result from the combustion of aluminized propellants are generally considered using simplified two phase flow models, due to a lack of experimental study or numerical methodologies for some of the more complicated physical processes involved. One such example is particle rotation; little study has been devoted to the effects of particle rotation in the flow regimes common to rocket exhaust plumes, and rotation has generally been neglected in plume modeling and analysis. In order to understand and quantify the influence of particle rotation on various flow properties, the mechanisms by which particles in the plume develop angular momentum must first be considered.

In a typical solid rocket motor, aluminum is used within the propellant grain to reduce combustion instabilities and increase specific impulse. Liquid alumina (Al_2O_3) droplets are formed inside the combustion chamber, with a bimodal size distribution concentrated around diameters of roughly 1 μm and 100 μm [1]. The droplets are then accelerated through the rocket nozzle, where they may encounter several different phenomena that tend to contribute angular momentum. First, smaller droplets are accelerated by the expanding gas far more rapidly than the larger droplets, so that droplets of different sizes develop widely varying velocities. Alumina droplets commonly account for 20% to 40% of the total mass flow through the nozzle entrance, so the high number density and considerable relative velocities between droplets of different sizes allow for a large number of collisions. Most of these collisions result in coalescence of the droplets into larger agglomerates, which rotate according to the dynamics of off-center coalescing collisions [2]. At the same time, larger droplets tend to break apart within the nozzle due to collisions or surface stresses imposed by the accelerating gas, and these breakup processes may impose significant angular momentum on the resulting droplet products. Within the subsonic converging nozzle region, larger droplets may diverge considerably from gas streamlines and accumulate in the boundary layers along the nozzle wall, where large transverse gradients in the bulk gas velocity can also induce rotation [3]. As the droplets cool and solidify into solid particles, inelastic collisions between particles may contribute to rotation as well. Turbulent and acoustic fluctuations in the gas can intensify many of these rotation mechanisms.

Report Documentation Page

Form Approved
OMB No. 0704-0188

1. REPORT DATE	2. REPORT TYPE	3. DATES COVERED
JUN 2004		**-**

4. TITLE AND SUBTITLE	5a. CONTRACT NUMBER
Particle Rotation Effects in Rarefied Two-Phase Plume Flows	5b. GRANT NUMBER
	5c. PROGRAM ELEMENT NUMBER

6. AUTHOR(S)	5d. PROJECT NUMBER
J Burt; I Boyd	**5503**
	5e. TASK NUMBER **000P**
	5f. WORK UNIT NUMBER

7. PERFORMING ORGANIZATION NAME(S) AND ADDRESS(ES)	8. PERFORMING ORGANIZATION REPORT NUMBER
Department of Aerospace Engineering,University of Michigan,Ann Arbor,MI,48109	

9. SPONSORING/MONITORING AGENCY NAME(S) AND ADDRESS(ES)	10. SPONSOR/MONITOR'S ACRONYM(S)
	11. SPONSOR/MONITOR'S REPORT NUMBER(S)

12. DISTRIBUTION/AVAILABILITY STATEMENT

Approved for public release; distribution unlimited

13. SUPPLEMENTARY NOTES

14. ABSTRACT

We evaluate the effects of solid particle rotation in high-altitude solid rocket exhaust plume flows, through the development and application of methods for the simulation of two phase flows involving small rotating particles and a nonequilibrium gas. GreenŸs functions are derived for the force, moment, and heat transfer rate to a rotating solid sphere within a locally free-molecular gas, and integration over a Maxwellian gas velocity distribution is used to determine the influence of particle rotation on the heat transfer rate at the equilibrium limit. The use of these GreenŸs functions for the determination of particle phase properties through the Direct Simulation Monte Carlo method is discussed, and a procedure is outlined for the stochastic modeling of interphase collisions. As a test case, we consider the nearfield plume flow for a Star-27 solid rocket motor exhausting into a vacuum, and vary particle angular velocities at the nozzle exit plane in order to evaluate the influence of particle rotation on various flow properties. Simulation results show that rotation may lead to slightly higher particle temperatures near the central axis, but for the case considered the effects of particle rotation are generally found to be negligible.

15. SUBJECT TERMS

16. SECURITY CLASSIFICATION OF:			17. LIMITATION OF ABSTRACT	18. NUMBER OF PAGES	19a. NAME OF RESPONSIBLE PERSON
a. REPORT	b. ABSTRACT	c. THIS PAGE			
unclassified	**unclassified**	**unclassified**		**6**	

In exhaust plume flows at high altitudes, the gas generally exhibits a high degree of nonequilibrium behavior outside of a small inviscid core region just beyond the nozzle exit [4]. The gas velocity and energy distributions can deviate significantly from the equilibrium limits, and continuum assumptions underlying Computational Fluid Dynamics (CFD) techniques may break down due to the large mean free paths in relation to the characteristic length scales for macroscopic flow gradients. In order to accurately model such flows, the nonequilibrium nature of the gas must therefore be considered within a non-CFD framework. As an additional problem in the consideration of two phase flows, typical CFD-based methods for two phase flow simulation use rarefaction corrections to empirical particle drag coefficient and Nusselt number formulations which often fail at the high Knudsen number and high Mach number conditions of interest.

As an alternative to empirical correlations for interphase momentum and energy transfer, analytical models for solid bodies in high Knudsen number flows may provide significant improvements in both overall accuracy and the physical effects which may be considered. Particle rotation is one such effect, and several authors have studied various properties associated with the rotation of objects within a free-molecular equilibrium gas. Epstein [5] derived the moment imparted on a rotating sphere, subject to several constraints including a lack of translational motion. Wang [6] determined the drag and lift coefficients for a rotating sphere, and showed that the direction of the lift force is opposite that of the Magnus force for continuum flow. Ivanov and Yanshin [7] derived force and moment equations for various bodies of revolution. While all of these authors have developed closed form solutions which are applicable to the general flow regimes of interest, the formulas they provide are limited by assumptions of Maxwellian gas velocity distributions, and none have considered the effect of rotation on interphase heat transfer. In addition, these formulas tend to be very complicated and poorly suited for evaluation within a larger numerical scheme for the simulation of high-altitude plume flows.

In a recent paper [8] a methodology is proposed for the simulation of such plume flows, where the gas is modeled using the Direct Simulation Monte Carlo (DSMC) method and the rates of momentum and heat transfer to the particles are based on equations of Gallis et al. [9] While the particles are assumed to be chemically inert, consideration is made for the effects of interphase momentum and energy transfer on both the particles and the gas. In the present effort, this method is extended to include effects of particle rotation, so that the influence of rotation on various flow properties can be evaluated. First, we derive the Green's functions for the force, moment and rate of heat transfer on a rotating spherical particle in a locally free-molecular gas. For the special case of a stationary rotating particle in a Maxwellian gas, the heat transfer Green's function is integrated analytically to provide a closed form solution. Next, we discuss the use of these Green's functions to modify the properties of representative solid particles within a two-phase DSMC simulation, and present two-way coupling approaches through which solid particles may influence the surrounding gas. When used within a larger two-phase flow model, these procedures allow for momentum and energy conservation in a time-averaged sense, and enable the simulation of two-phase rarefied flows involving very large solid particle mass fractions.

The procedures mentioned above are implemented for two phase flow calculations in the DSMC code MONACO [10]. As a test case, we consider the near-field plume flow for a Star-27 solid rocket motor [11] exhausting into a vacuum. Estimates of particle angular velocities at the nozzle exit are based on the assumption that coalescing droplet collisions within the nozzle are the dominant mechanism for inducing particle rotation, and calculations are made using the limiting cases of maximum possible and zero initial angular velocities. Comparison of results shows that, at least for the case considered, effects associated with particle rotation are generally within the limits of statistical scatter in the calculated flow properties.

ANALYSIS OF ROTATION EFFECTS

Following the Green's function approach of Gallis et al. [9], we consider a spherical solid particle within a locally free-molecular simple gas. Incident gas molecules which collide with the particle are either specularly reflected off the surface, or are diffusely reflected with full thermal accommodation of translational and rotational energy modes to the particle temperature. We assume that the particle is small enough to allow for a low-Biot number approximation of spatially uniform temperature, yet large enough that the change in particle velocity during an interphase collision is much smaller than that of the gas molecule. These assumptions are all generally valid for the high altitude plume flows of interest, and are used to derive the following Green's function for the force on a nonrotating particle due to gas molecules of relative velocity class $\mathbf{u}_r$:

$$\mathbf{F}_{nr}(\mathbf{u}_r) = \pi R_p^2 n_g f(\mathbf{u}_r) \left(m c_r + \frac{\tau}{3} \sqrt{2\pi m k_B T_p} \right) \mathbf{u}_r \qquad (1)$$

Here R_p is the particle radius, n_g is the gas number density, $f(\mathbf{u}_r)$ is the gas velocity distribution function in a particle-centered coordinate frame, m is the mass per gas molecule, c_r is the relative speed, τ is the particle thermal accommodation coefficient, T_p is the particle temperature and k_B is Boltzmann's constant.

In considering the Green's function $\mathbf{F}_p(\mathbf{u}_r)$ for the force imparted by the gas on a rotating particle, we first decompose $\mathbf{F}_p$ into a term which accounts for momentum transfer to the particle from incident gas molecules, a term for momentum exchange during specular reflection, and a corresponding term for diffuse reflection. It can be shown that the second term is zero and that only the third term may be influenced by particle rotation. Next, using the velocity superposition principle, the momentum transfer due to diffuse reflection is separated into a component independent of rotation and a component which depends on the particle angular velocity $\boldsymbol{\omega}_p$ but is independent of T_p. This latter component is the only contributor in a time-averaged sense to the force Green's function $\mathbf{F}_{rot}$ due to particle rotation, and allows the Green's function for the total force on the particle to be computed as $\mathbf{F}_p = \mathbf{F}_{nr} + \mathbf{F}_{rot}$. Following the above logic, $\mathbf{F}_{rot}$ is equal to the product of the collision frequency for diffusely reflecting collisions and the rotational component $-m\langle\mathbf{u}_t\rangle$ of the average momentum transferred to the particle during diffuse reflection. Here $\mathbf{u}_t$ is the tangential velocity of the particle surface at the collision point in an inertial particle-centered reference frame. In order to evaluate $\langle\mathbf{u}_t\rangle$ we express $\mathbf{u}_t$ as a function of the angle θ between $-\mathbf{u}_r$ and the outward surface normal unit vector $\mathbf{n}_c$ at the collision point, then multiply by the distribution function for θ and integrate over all particle surface elements where a collision may occur. We find:

$$\mathbf{F}_{rot}(\mathbf{u}_r) = \frac{2\pi}{3} R_p^3 m n_g f(\mathbf{u}_r) \tau \, \boldsymbol{\omega}_p \times \mathbf{u}_r \tag{2}$$

By adding (1) and (2) and integrating over all gas velocity space, we then determine the total force on the particle.

In the absence of any gas vorticity effects or forces not associated with interphase collisions, the rotating particle will experience a damping moment about the particle center which will tend over time to reduce the magnitude of $\boldsymbol{\omega}_p$. Depending on the angle between $\boldsymbol{\omega}_p$ and the gas bulk velocity relative to the particle, the moment may also have a component orthogonal to $\boldsymbol{\omega}_p$ which tends to change the axis about which the particle rotates. This moment can be determined using the same Green's function approach as above. Again, incident and specularly reflected gas molecules do not contribute to the moment, and the average moment contribution during diffuse reflection depends only on the tangential velocity of the particle surface. The Green's function $\mathbf{M}_p(\mathbf{u}_r)$ for this moment can then be expressed as the negative product of the collision frequency for diffuse reflection and the average angular momentum $mR_p\langle\mathbf{n}_c \times \mathbf{u}_t\rangle$ about the particle center imparted on diffusely reflected gas molecules. The averaging operation is performed through integration over the particle surface, to find the following result:

$$\mathbf{M}_p(\mathbf{u}_r) = \frac{1}{4}\pi R_p^4 m n_g f(\mathbf{u}_r) \tau c_r \left(\frac{\mathbf{u}_r \cdot \boldsymbol{\omega}_p}{c_r^2} \mathbf{u}_r - 3\boldsymbol{\omega}_p \right) \tag{3}$$

Through energy conservation arguments, the Green's function for the heat transfer rate to a rotating particle can be expressed as

$$\dot{Q}_p(\mathbf{u}_r) = \pi R_p^2 n_g f(\mathbf{u}_r) \tau c_r \left[\frac{1}{2} m c_r^2 - e_{kin} + \left(e_{rot} - \frac{1}{2} \Lambda_{rot} k_B T_p \right) \right] - \mathbf{M}_p(\mathbf{u}_r) \cdot \boldsymbol{\omega}_p \tag{4}$$

where e_{rot} is the average rotational energy of incident gas molecules, Λ_{rot} is the number of rotational degrees of freedom for the gas, and $e_{kin} = 2k_B T_p + \tfrac{1}{2} m\langle\mathbf{u}_t \cdot \mathbf{u}_t\rangle$ is the average kinetic energy of diffusely reflected gas molecules in an inertial particle-fixed coordinate frame. By integrating over the particle surface, we derive the general formula

$$\dot{Q}_p(\mathbf{u}_r) = \pi R_p^2 n_g f(\mathbf{u}_r) \tau c_r \left[\frac{1}{2} m c_r^2 - \left(2 + \frac{1}{2} \Lambda_{rot} \right) k_B T_p + e_{rot} + \frac{1}{8} m \omega_p^2 R_p^2 \left(3 - \frac{(\mathbf{u}_r \cdot \boldsymbol{\omega}_p)^2}{c_r^2 \omega_p^2} \right) \right] \tag{5}$$

where $\omega_p = |\boldsymbol{\omega}_p|$. Note from (5) that a greater value of ω_p corresponds to an increase in heat transfer from the gas to the particle. This property can be justified physically by considering a single particle surface element in a coordinate frame which is fixed to the local tangential surface velocity. In this coordinate frame the average kinetic energy of diffusely reflected gas molecules will be independent of ω_p, while the average kinetic energy of incident gas molecules tends to increase as ω_p^2. Thus, the only effect of particle rotation here is to increase the interphase energy transfer associated with the kinetic energy of incident gas molecules which are involved in diffusely reflecting collisions.

In the special case where the particle which moves at the bulk velocity of an equilibrium simple gas with temperature T_g, (5) may be integrated analytically over all gas velocity space to provide a closed form solution for the net heat transfer rate:

$$\dot{Q}_{p,\,net} = R_p^2\, n_g\, \tau \sqrt{2\pi k_B T_g / m}\left[\left(4+\Lambda_{rot}\right) k_B\left(T_g - T_p\right) + \frac{2}{3} m \alpha_p^2 R_p^2\right] \tag{6}$$

If $T_p > T_g$ as is typical for high-altitude rocket exhaust plume flows, then the two bracketed terms in (6) are of opposite sign. Assuming the first term is greater in magnitude than the second, we find that particle rotation tends to reduce the magnitude of the heat transfer rate and allows for a more gradual reduction in T_p over time.

DSMC IMPLEMENTATION

The Green's functions given above can be used to allow rotating solid particles to be modeled within a DSMC simulation. For simplicity we neglect radiative heat transfer and assume the particle phase to be dilute and chemically inert, so that temporal variation in the properties of individual particles may occur only through the mechanisms described above or through particle-wall interactions. Representative solid particles are tracked along with DSMC gas molecules through a computational grid, and during each time step the total force, moment, and heat transfer rate for each particle is determined by adding contributions from all gas molecules which are assigned to the same cell. The force, moment and heat transfer contributions to a particle from a single DSMC gas molecule are computed by evaluating (1), (2), (3) and (5) with the quantity $n_g f(\mathbf{u}_r)$ replaced by the ratio of the local gas molecule weighting factor to the cell volume. Once all N_g molecules in the cell have been considered, the particle velocity $\mathbf{u}_p$ and temperature T_p are altered as described in Ref. [8], and $\boldsymbol{\omega}_p$ is updated by the product of the net moment, the local time step and the inverse of the particle moment of inertia.

Due to the large particle phase mass fractions typical of the high-altitude plume flows of interest, accurate simulation requires consideration of momentum and energy coupling from the particles to the gas. This is accomplished here by probabilistically modeling individual interphase collisions and modifying the velocity and rotational energy of all gas molecules involved. A collision selection scheme based on the No Time Counter method of Bird [12] is used to determine which, if any, DSMC gas molecules will collide with each solid particle during a given time step. If a particular gas molecule is found to collide with the particle, then the collision will involve either diffuse reflection, with probability τ, or specular reflection, with probability $1-\tau$. In the latter case, the post-collision relative velocity $\mathbf{u}_r^*$ is sampled from an isotropic distribution such that the relative speed c_r of the molecule is unchanged during the collision, and the molecule velocity is reassigned to equal $\mathbf{u}_p+\mathbf{u}_r^*$. In the case of diffuse reflection, a more complicated procedure is required to find $\mathbf{u}_r^*$, and the gas molecule rotational energy must be altered as well.

If a gas molecule is diffusely reflected off a nonrotating solid particle, then the magnitude and direction of $\mathbf{u}_r^*$ are statistically independent, so each can be determined separately. Following the procedure outlined in Ref. [8], the post-collision relative speed c_r^* is sampled from the distribution function

$$f(c_r^*)\,dc_r^* = 2\beta_p^4 c_r^{*3} \exp(-\beta_p^2 c_r^{*2})\,dc_r^* \tag{7}$$

using the acceptance-rejection method [12], where $\beta_p = \sqrt{m/(2k_B T_p)}$. The angle δ between the vectors $-\mathbf{u}_r$ and $\mathbf{u}_r^*$ is also determined using the acceptance-rejection method, by sampling from a numerical approximation

$$f(\delta) = 0.02042\delta^6 - 0.2515\delta^5 + 1.104\delta^4 - 1.903\delta^3 + 0.4938\delta^2 + 1.248\delta \tag{8}$$

of the distribution function for $\delta \in [0, \pi]$. An azimuthal angle α_0 required to define the direction of $\mathbf{u}_r^*$ in three dimensional space is sampled from a uniform distribution over $[0, 2\pi]$, and the components of $\mathbf{u}_r^*$ are calculated using formulas derived by Bird [12] for binary elastic collisions:

$$u_r^* = \frac{c_r^*}{c_r}\left[-u_r\cos\delta + \sin\delta\sin\alpha_0\left(v_r^2+w_r^2\right)^{1/2}\right],\quad v_r^* = \frac{c_r^*}{c_r}\left[-v_r\cos\delta - \frac{\sin\delta\left(c_r w_r \cos\alpha_0 + u_r v_r \sin\alpha_0\right)}{\left(v_r^2+w_r^2\right)^{1/2}}\right],\quad w_r^* = \frac{c_r^*}{c_r}\left[-w_r\cos\delta + \frac{\sin\delta\left(c_r v_r \cos\alpha_0 - u_r w_r \sin\alpha_0\right)}{\left(v_r^2+w_r^2\right)^{1/2}}\right] \tag{9}$$

The absolute velocity of the gas molecule is then set to the final value $\mathbf{u}_p+\mathbf{u}_r^*$.

If a diffusely reflecting collision involves a rotating solid particle, then Eq. 8 is not valid and an alternate procedure must be used. In this case $\mathbf{u}_r^*$ is found by separately determining nonrotational $\mathbf{u}_{nr}^*$ and rotational $\mathbf{u}_{rot}^*$ components, then adding the two together. To calculate $\mathbf{u}_{nr}^*$, we first compute the angle θ between $-\mathbf{u}_r$ and the outward normal unit vector $\mathbf{n}_c$ at the collision point on the particle surface by setting $\sin^2\theta$ equal to a random number on [0, 1]. A corresponding azimuthal angle α_1 is sampled from a uniform distribution over $[0, 2\pi]$, and components of $\mathbf{n}_c$ are then calculated as

$$n_{c,x} = \frac{1}{c_r}\left[-u_r\cos\theta + \sin\theta\sin\alpha_1\left(v_r^2+w_r^2\right)^{1/2}\right],\quad n_{c,y} = \frac{1}{c_r}\left[-v_r\cos\theta - \frac{\sin\theta\left(c_r w_r \cos\alpha_1 + u_r v_r \sin\alpha_1\right)}{\left(v_r^2+w_r^2\right)^{1/2}}\right],\quad n_{c,z} = \frac{1}{c_r}\left[-w_r\cos\theta + \frac{\sin\theta\left(c_r v_r \cos\alpha_1 - u_r w_r \sin\alpha_1\right)}{\left(v_r^2+w_r^2\right)^{1/2}}\right]. \tag{10}$$

Next, we find the angle ζ between the vectors $\mathbf{n}_c$ and $\mathbf{u}_{nr}^*$ by sampling $\sin^2\zeta$ from a uniform distribution over [0, 1]. An azimuthal angle α_2 is sampled from a uniform distribution over [0, 2π], and Eq. 7 is used to find the magnitude of $\mathbf{u}_{nr}^*$. The components of $\mathbf{u}_{nr}^*$ are then determined through the following equations:

$$u_{nr}^* = c_r^* \left[n_{c,x}\cos\zeta + \sin\zeta \sin\alpha_2 (1-n_{c,x}^2)^{1/2} \right], \quad v_{nr}^* = c_r^* \left[n_{c,y}\cos\zeta + \frac{\sin\zeta (n_{c,z}\cos\alpha_2 - n_{c,x} n_{c,y} \sin\alpha_2)}{(1-n_{c,x}^2)^{1/2}} \right], \quad w_{nr}^* = c_r^* \left[n_{c,z}\cos\zeta - \frac{\sin\zeta (n_{c,y}\cos\alpha_2 + n_{c,x} n_{c,z} \sin\alpha_2)}{(1-n_{c,x}^2)^{1/2}} \right] \quad (11)$$

Finally, the rotational component of $\mathbf{u}_r^*$ is computed as $\mathbf{u}_{rot}^* = R_p\, \boldsymbol{\omega}_p \times \mathbf{n}_c$, and the gas molecule velocity is reassigned to the post-collision value $\mathbf{u}_p + \mathbf{u}_{nr}^* + \mathbf{u}_{rot}^*$.

PLUME SIMULATION

To evaluate the importance of particle rotation effects, all procedures described above are implemented in the DSMC code MONACO [10], and an axisymmetric simulation is performed for the nearfield plume flow from a Star-27 solid rocket motor expelling into a vacuum. The nozzle has an exit diameter of 78 cm and a divergence half-angle of 17.2°. All gas and particle properties along the nozzle exit plane are taken from Anfimov et al. [11] Based on values provided by these authors, spherical Al_2O_3 particles of diameter D_p = 0.15, 0.2, 0.3, 0.5, 1, 2 and 3 μm together constitute a total mass flow fraction of about 30%, with particles of each size distributed uniformly over the nozzle exit. The gas here is a mixture of H_2, N_2 and CO, with mole fractions of 0.38, 0.31, and 0.31 respectively. Effects of radiative heat transfer, heterogeneous reactions, gas chemistry and particle phase change are neglected. While each of these phenomena may significantly alter flow properties of interest, we intend only to assess the importance of particle rotation effects on a representative plume flow, not to calculate flow properties for a particular case with the greatest possible accuracy.

Following Vasenin et al. [2], we assume that coalescing collisions between liquid droplets within the nozzle are the dominant contributors to particle rotation. The maximum allowable particle angular velocity magnitude is then determined by a criterion for the centrifugal breakup of liquid droplets. A normalized angular velocity

$$\Omega = \frac{4}{5}\,\omega_p \sqrt{\frac{\pi}{3}\frac{m_p}{\sigma}} \quad (12)$$

is set to equal some critical value Ω_{crit} for all particles at the nozzle exit, where m_p is the particle mass and σ is the liquid surface tension of the particle material. While the magnitude of $\boldsymbol{\omega}_p$ will be constant for all particles of equal diameter at the nozzle exit, the initial direction of $\boldsymbol{\omega}_p$ for each particle is randomly selected on a plane normal to the axis of symmetry. Salita [1] uses momentum and energy conservation arguments to show that the collision-induced rotation rate of spherical liquid agglomerates should be limited by Ω_{crit}=3.31. Following these arguments, we perform plume simulations with initial particle angular velocities corresponding to Ω=3.31 and Ω=0 in order to evaluate potential upper bounds for the influence of particle rotation on various flow properties. For both cases, particle-to-gas coupling is considered through application of the method described above involving (10) and (11), to avoid any differences in results caused by the numerical approximation in (8).

The simulations use a rectangular grid domain, starting at the nozzle exit plane and extending 10 m downstream in the axial direction and 4 m in the radial direction. Calculations are performed on 16 1.4 GHz AMD Opteron processors, with each case requiring about 3000 CPU hours. As an example of simulation results for the Ω=3.31 case, Figure 1 shows average angular velocity magnitudes for particles of each size as a function of distance from the central axis, along a radial plane 10 m downstream of the nozzle exit. Figure 2 shows the variation in average particle temperatures along this same plane, for both the Ω=3.31 and Ω=0 cases. From a comparison of T_P values for any radial location and particle size, particle rotation is shown in Figure 2 to have little measurable impact on particle temperatures in the plume. However, for all but the largest and smallest particles considered, rotation does account for a roughly 5 to 10 K increase in average particle temperatures within about 0.5 m of the central axis. This trend is likely due to the fact that the gas density, and therefore the component of the interphase energy transfer rate associated with particle rotation, tends to decrease with distance from the axis. The trend is less pronounced for the smallest particles because these rapidly lose the bulk of their rotational energy on entering the grid domain, and for the largest particles because of their relatively low initial angular velocities.

With this one minor exception, we find a general lack of dependence on particle rotation for all flow properties of interest. Distributions of gas translational temperature, particle and gas number densities, maximum divergence angles for each particle size, and various other properties show differences between the two cases which are comparable to the expected statistical scatter. We can therefore conclude that, at least for the plume simulation

considered here, particle rotation may be neglected with no significant loss in overall accuracy. The numerical methods described above do maintain some utility in making this conclusion possible, and in allowing for the simulation of other two-phase rarefied flows, such as MEMS flows involving frequent particle-wall collisions, where rotation effects may still be important.

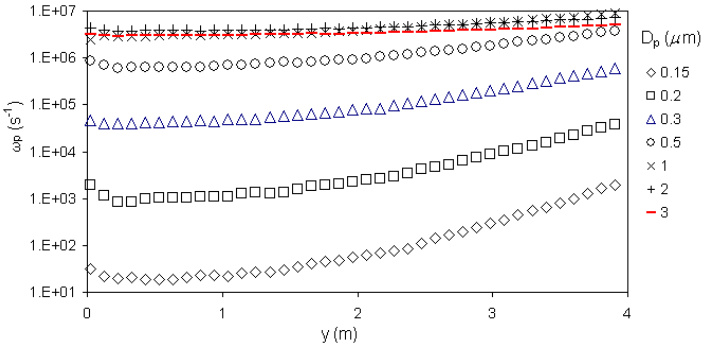

FIGURE 1. Variation in particle angular velocity magnitudes along a radial plane 10 m downstream from the nozzle exit.

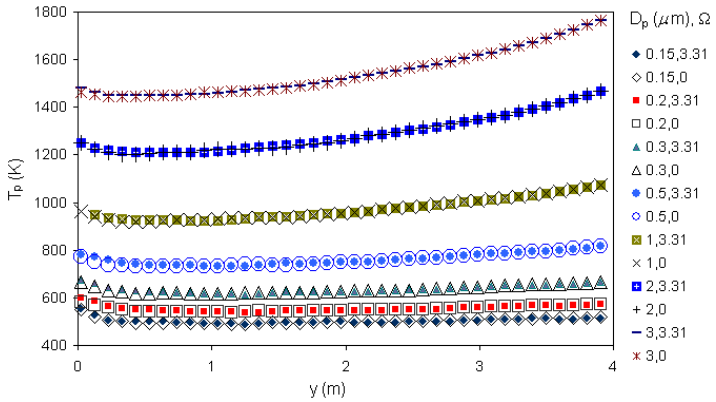

FIGURE 2. Average particle temperature as a function of distance from the central axis.

ACKNOWLEDGMENTS

The authors gratefully acknowledge financial support for this work from the Air Force Research Laboratory at Edwards Air Force Base, with Dean Wadsworth and Tom Smith as technical monitors.

REFERENCES

1. Salita, M., J. Propulsion and Power 7, 505-512 (1991).
2. Vasenin, I. M., Narimanov, R. K., Glazunov, A. A., Kuvshinov, N. E., and Ivanov, V. A., J. Propulsion and Power 11, 583-592 (1995).
3. Crowe, C., Sommerfeld, M., and Tsuji, Y., Multiphase Flows with Droplets and Particles, CRC, New York, 1998, p. 99.
4. Simmons, F. S., Rocket Exhaust Plume Phenomenology, Aerospace Press, El Segundo, CA, 2000, pp.21-30.
5. Epstein, P. S., Phys. Review 24, 710-732 (1924).
6. Wang, C., AIAA Journal 10, 713-714 (1972).
7. Ivanov, S. G., and Yanshin, A. M., Fluid Dynamics 15, 449-453 (1980).
8. Burt, J. M., and Boyd, I. D., AIAA Paper 2004-1351 (2004).
9. Gallis, M. A., Torczynski, J. R., and Rader, D. J., Physics of Fluids 13, 3482-3492 (2001).
10. Dietrich, S., and Boyd, I. D., J. Computational Physics 126, 328-342 (1996).
11. Anfimov, N. A., Karabadjak, G. F., Khmelinin, B. A., Plastinin, Y. A., and Rodionov, A. V., AIAA Paper 93-2818 (1993).
12. Bird, G. A., Molecular Gas Dynamics and the Direct Simulation of Gas Flows, Clarendon Press, Oxford, 1994, pp. 34-36, 218-220, 425.